Extracellular matrix hyaluronan modulates fat cell differentiation and primary cilia dynamics

Krzysztof Drygalski, Romane Higos, Fatiha Merabtene, Patrycja Mojsak, Kamil Grubczak, Michal Ciborowski, Hady Razak, Karine Clément, Isabelle Dugail

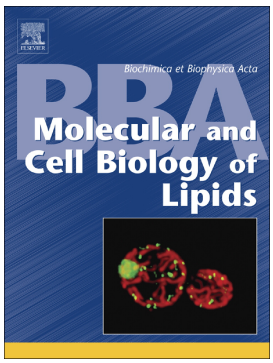

Extracellular matrix hyaluronan modulates fat cell differentiation and primary cilia dynamics

Krzysztof Drygalski, Romane Higos, Fatiha Merabtene, Patrycja Mojsak, Kamil Grubczak, Michal Ciborowski, Hady Razak, Karine Clément, Isabelle Dugail

PII: S1388-1981(24)00020-9

DOI: https://doi.org/10.1016/j.bbalip.2024.159470

Reference: BBAMCB 159470

To appear in: *BBA - Molecular and Cell Biology of Lipids*

Received date: 4 December 2023

Revised date: 2 February 2024

Accepted date: 26 February 2024

Please cite this article as: K. Drygalski, R. Higos, F. Merabtene, et al., Extracellular matrix hyaluronan modulates fat cell differentiation and primary cilia dynamics, *BBA - Molecular and Cell Biology of Lipids* (2023), https://doi.org/10.1016/j.bbalip.2024.159470

Extracellular matrix Hyaluronan modulates fat cell differentiation and primary cilia dynamics.

Krzysztof Drygalski[1,2], Romane Higos[1], Fatiha Merabtene[1], Patrycja Mojsak[3], Kamil Grubczak[4], Michal Ciborowski[3], Hady Razak [5], Karine Clément[1,6], Isabelle Dugail[1]

[1]INSERM, Sorbonne Université, NutriOmics team : Nutrition/Obesities- systemic approaches, Paris 75013, France.
[2]Department of Hypertension and Diabetology, Medical University of Gdansk, 80-210 Gdansk, Poland
[3]Clinical Research Centre, Medical University of Bialystok, 15-276 Białystok, Poland
[4]Department of Regenerative Medicine and Immune Regulation, Medical University of Bialystok, 15-269 Bialystok, Poland
[5]Department of General and Endocrine Surgery, Medical University of Bialystok, 15-276 Bialystok, Poland
[6]Assistance Publique-Hopitaux de Paris, Nutrition department, Pitié-Salpetrière Hospital, 75013 Paris, France
Corresponding author : isabelle.dugail@inserm.fr

Short title: Inhibition of adipocyte differentiation by Haluronidase

Funding sources: This work was supported by the Polish Ministry of Sciences and Higher Education within the Diamond Grant 2019 program (no. DI2018 025448). Nutriomics team is supported by a grant from Fondation pour la recherche medicale (FRM Team 2020-2023). ID received support from Fondation de France.

Key words : Lipid storage, adipocyte, 3T3L1, preadipocytes.

Abstract (230 words)

Hyaluronan is an important extracellular matrix component, with poorly documented physiological role in the context of lipid-rich adipose tissue. We have investigated the global impact of hyaluronan removal from adipose tissue environment by *in vitro* exposure to exogenous hyaluronidase (or heat inactivated enzyme). Gene set expression analysis from RNA sequencing revealed downregulated adipogenesis as a main response to hyaluronan removal from human adipose tissue samples, which was confirmed by hyaluronidase-mediated inhibition of adipocyte differentiation in the 3T3L1 adipose cell line. Hyaluronidase exposure starting from the time of induction with the differentiation cocktail reduced lipid accumulation in mature adipocytes, limited the expression of terminal differentiation marker genes, and impaired the early induction of co-regulated *Cebpa* and *Pparg* mRNA. Reduction of *Cebpa* and *Pparg* expression by exogenous hyaluronidase was also observed in cultured primary preadipocytes from subcutaneous, visceral or brown adipose tissue of mice. Mechanistically, inhibition of adipogenesis by hyaluronan removal was not caused by changes in osmotic pressure or cell inflammatory status, could not be mimicked by exposure to threose, a metabolite generated by hyaluronan degradation, and was not linked to alteration in endogenous Wnt ligands expression. Rather, we observed that hyaluronan removal associated with disrupted primary cilia dynamics, with elongated cilium and higher proportions of preadipocytes that remained ciliated in hyaluronidase-treated conditions. Thus, our study points to a new link between ciliogenesis and hyaluronan impacting adipose tissue development.

Introduction

The extracellular matrix (ECM) provides a rigid frame on which cells anchor for tissue shaping. It plays multiple roles from regulating cell mobility and migration, signaling mechanical clues to the cell interior, and modulating intercellular cross talks. The adipose tissue ECM scaffold has special importance for tissue architecture because adipocytes are uniquely large (100µm diameter or more) and have low rigidity due to their outstandingly high triglyceride content. Moreover, fat cells continuously adapt their size according to nutritional state through shrinking/expansion changes in lipid stores, which suggests that ECM mechanical forces exerted to and from the adipocytes highly fluctuate according to metabolic conditions. Accordingly, adipocyte metabolic responses to ECM-derived mechanical forces have been reported (1). Adipose tissue ECM consists mainly in common constituents such as fibrillary proteins (collagens, fibronectin) and glycosaminoglycans (hyaluronan) filaments to which many other non-fibrillary matricellular proteins can associate, but it has not been exhaustively analyzed.

Only few adipose-derived ECM components have documented roles on fat tissue lipid storage. For example, mice with adipocyte-specific deficiency in Collagen VI expression (Ad-Col6-KO) were characterized for an outstanding capacity in adipose tissue expansion when faced lipid rich diets (2). Ad-Col6-KO mice, can reach a body weight that is twice that of wild type animals fed the same high fat diet, providing evidence that ECM rigidity limits fat cell expandability and lipid storage. Another documented example is beneficial Hyaluronan production by mature adipocytes, which has been unraveled using a mouse model with inducible adipocyte-specific overexpression of Hyaluronan Synthase2 (Ad-HAS2 Ovex). These mice were found to resist high fat diet induced obesity, to have smaller adipocytes and to be less glucose intolerant (3), indicating that adipose tissue Hyaluronan might exert beneficial metabolic actions. In line, one study by Ji and colleagues has reported that limitation of Hyaluronan extracellular deposition by pharmacological 4MU-induced inhibition of Hyaluronan synthesis had similar anti-adipogenic effects than extracellular degradation with exogenous Hyaluronidase exposure (4). In agreement, Hyaluronidase infusion *in vivo* could block the process of reactive adipogenesis that relates to the formation of fat tissue around injured colon or skin (5). Thus, adipose Hyaluronan appears to modulate lipid storage though fat cell differentiation, but the underlining mechanisms remain unexplored.

It is obvious that lipid excess in obesity associates with is highly remodeled adipose tissue ECM, in connection with low grade inflammation that develops in chronically lipid-laden adipose tissue (6). With worsening obesity, ECM accumulates to ultimate adipose tissue fibrosis with collagen accretion (7). The scoring of collagen accumulation defines degrees of adipose tissue fibrosis (8), associated with poor metabolic health in patients (9). Adipose tissue fibrosis is also highly predictive for a poor response to weight loss induced by bariatric surgery (10). Such clinical observations underscore the need for more information on adipose tissue ECM in health and disease conditions.

Although multiple cell types within adipose tissue can produce ECM components, the role of a specific adipose progenitors population called fibro-inflammatory progenitors expressing high levels of Ly6C and Cd9 has been demonstrated in obesity-related adipose tissue fibrosis (11)(12), and during chronic TGFb activation (13). Interestingly, the pro-fibrotic activity of adipose progenitors is reduced by agents that orient their differentiation capacity towards an adipose brown-like phenotype with thermogenic potential (14). It was also demonstrated that macrophages have ECM degradative activity, a process that is dependent on their anti-inflammatory M2 like phenotype (15).

We wished to characterize the contribution of Hyaluronan in the context of adipose tissue ECM. Hyaluronan is a high molecular weight polymeric glycosaminoglycan chain formed by repetition of disaccharide units, devoid of any protein component. It has unique physical properties and can form a highly hydrophilic gel, which participates in extracellular osmotic pressure and tissue hydratation. Despite its wide utilization as a filling material in tissue reconstruction and esthetic surgery, little is known on Hyaluronan role as an ECM component in the lipid-enriched adipose tissue.

In the present study, we investigated the impact of extracellular hyaluronan removal from the adipose tissue microenvironment by using exogenous hyaluronidase (HAse). We started from unbiased metabolomics and RNA Sequencing approaches on adipose tissue fragments, which confirmed modulation of adipogenesis. Indeed, ECM hyaluronan degradation strongly inhibited differentiation of the 3T3L1 adipose cell line and that of preadipocytes isolated from mouse adipose depots grown in primary culture. We have used the 3T3L1 as a model for adipocyte conversion to investigate potential mechanisms responsible for hyaluronidase-mediated inhibition of fat differentiation, and could exclude several potential candidates like inflammation, extracellular osmotic pressure, Wnt signaling activation, or antiadipogenic actions possibly exerted by hyaluronan-derived sugar metabolites. Instead, we found that extracellular hyaluronan removal associated with elongated preadipocyte primary cilia, and restrained cilia disassembly that is required for fat cell differentiation to proceed.

Materials and methods

Adipose tissue collection for Metabolomics: Adipose tissue was collected from three lean patients without active inflammation undergoing elective strumectomy or hernioplasty. All the procedures were conducted by the same operating team upon the permission of Ethical Committee at Medical University of Bialystok R-I-002/478/2018. Subcutaneous adipose tissue (SCAT) fragments (single piece of approximately 5x5x5mm) were placed in ice-cold phosphate buffered saline and immediately transported to the laboratory. Each fragment was embedded in warm 4% agarose in PBS buffer so that about 2-4 mm thick agarose layer is left around the tissue. Once settled, the agarose blocks were cut on a Leica VT1200S vibrating microtome with optimized cutting conditions (1-1.2mm/s of cutting speed, 1.5mm amplitude of blade vibration and 500µm slice thickness). Subsequently, slices were placed on 12-well plate in 1ml of growth medium (DMEM high glucose/ without pyruvate +10% fetal bovine serum (FBS) +1%pennicilin/streptomycin) for 1-2h in a humidified incubator with 5% CO_2/95% air at 37^{o}C until exposure to exogenous Hyaluronidase for 24h. After incubation, slice homogenates were collected and prepared for untargeted metabolomics. Metabolites were identified by GC-MS analysis with subsequent data processing as previously described (16,17).

RNA sequencing: RNA isolated from adipose tissue explants was sent for library preparation and Next Generation Sequencing using Illumina platform in external company (Eurofins, Germany). Genes receiving less than 10 reads on an average across the compared groups were removed. The abundance counts of each gene were then used to perform differential gene expression (DGE). DGE was performed using R/Bioconductor DESeq2 (18) package, which essentially normalizes the abundance counts to account for observed variance (due to differences in sequencing depths, sample groups and replicates) generating normalized gene counts. Statistical tests were performed to compare the distributions between conditions (treatment vs control) generating p-values for each gene. The final p-values were corrected by determining false discovery rates (FDR) using the Benjamin–Hochberg method. Using a FDR

corrected p-value (adjusted p-value) <0.1 as a threshold, significantly differentially expressed genes between conditions were identified and reported.

Cell culture: 3T3L1 cell line (originally provided by J. Pairault) was maintained frozen in liquid nitrogen. Cells were propagated in a fibroblastic state in high glucose DMEM supplemented with 10% fetal bovine serum and 1% Penicillin/Streptomycin, and induced to differentiate when confluent in the presence of a differentiation cocktail containing Isobutyl-methylxanthine/Dexamethasone/Insulin) as described previously (19). Hyaluronidase (HAse from bovine testis, 400µg/ml in PBS, Sigma Aldrich, #H3506) was added to the medium from confluence and renewed at every medium change. Control cells received either vehicle alone (PBS) or heat inactivated Hyaluronidase treated for 15 min at 95°C (hiHAse). In some experiments, primary progenitors from the stroma-vascular fraction of mouse adipose tissue were grown in culture as described in (14) and were exposed to HAse (or heat inactivated enzyme) from Day 1 after seeding.

Agarose gel electrophoresis for Hyaluronan imaging: For hyaluronan extraction, cells and medium were scraped in 1X proteinase K (Macherey Nagel, #74095.250) and incubated 4 hours at 60℃ followed by overnight precipitation in 100% ethanol at -20℃. After centrifugation, pellets were resuspended in ammonium acetate and incubated for 20 minutes before boiling to deactivate proteinase K. Then, DNase (Macherey Nagel, #740963) and RNase (120 U/mg, Macherey Nagel, #740505) were added at 1uL for 20uL of sample each, and incubated for 4 hours at 37℃. Following a second overnight ethanol precipitation, samples were centrifuged 20 minutes at 4000g and the pellet was resuspended in ultrapure water. A 0.5% agarose gel was prepared in 1X TAE buffer and pre-runned at 150V in 1X TAE buffer before loading samples (10µl mixed with 5uL of loading buffer (Invitrogen, #10816015). Calibrated Hyaluronan markers (Hyalose Inc., HYA-HiLAD-20) and a 1Kb DNA ladder (Invitrogen, #10787018) were loaded for size calibration. The gel was then transferred to 0.002% StainsAll solution (Sigma, #E9379) in 50% Ethanol and left to incubate in the dark at room temperature. After 24 hours, the gel was rinced with 10% ethanol in the dark. Once the gel had stopped floating, it was exposed to even white light and pictures were taken after de-staining was complete.

RT-qPCR mRNA analysis. RNA was extracted from cultured cells, and used for RT-QPCR analysis as described (14).

Cell imaging: Cell lipid accumulation was visualized with LipidTox™ (ThermoFisher Scientific) staining of living cells as recommended by manufacturer, or by staining with Oil red O (Sigma, #O0625).

Immunofluorescence staining for cilia imaging: Cells were seeded on glass coverslips and induced to differentiate with standard protocol in the presence or absence of HAse. Serum was withdrawn from the medium 24 hours before cell fixation (10 min in 3.7% PFA followed by 10 min permeabilization with 0.1% Triton-X100 in PBS). After blocking for 30 minutes with 3% foetal bovine serum and 0.1% Tween-20 in PBS, cells were incubated for 2 hours with primary antibody (Rabbit polyclonal anti Arl13b Proteintech, #17711-1) diluted in DMEM +10% FBS, followed by 1 hour with secondary antibody (anti rabbit Dylight 488) in the same buffer. Coverslips were mounted on microscope slides with Fluoromount G with DAPI (Invitrogen, #00-4959-52). Z stack images were obtained with a Leica SP8 DLS inverted microscope. Total numbers of nuclei and cilia as well as cilia length were manually determined using Image J software.

Statistical analysis: Metabolomics data were analyzed using Metaboanalyst software (https://www.metaboanalyst.ca/). RNA seq raw data obtained from Eurofins Genomics GmbH were

processed for Gene Set Enrichment Analysis (GSEA) using the algorithm developed by Broad Institute/UC San Diego, described in (20). For other data analysis, paired Student's t test was used to evaluate the statistical significance of the impact of HAse treatment, at a threshold of $p<0.05$. At least 3 independent experiments were analyzed.

Results

To document the role of Hyaluronan as an adipose tissue ECM component, we investigated the impact of its extracellular removal from the tissue environment using exogenous hyaluronidase (HAse). Subcutaneous adipose tissue biopsies obtained from 3 healthy lean subjects were maintained in serum-supplemented DMEM containing or not exogenous HAse (0.4 mg/ml, for 24 hours) prior to analysis by metabolomics and RNA-seq technologies. Preliminary experiments performed on cultured 3T3L1 adipocytes, a validated model for fat cells ensured that a 24h-incubation with exogenous HAse was able to decrease extracellular Hyaluronan contents with high efficiency, validated by agarose staining with the "Stains all" dye reagent which reveals Hyaluronan in blue, nucleic acids in violet and proteoglycans in brown. We observed strong blue-colored Hyaluronan smears highly produced in the culture medium of 3T3L1 adipocytes, that resisted exposure to heat inactivated HAse and almost undetectable proteoglycans **(Fig 1A)**. Further, when applied at any time point during the differentiation process of 3T3L1 adipocytes, exogenous HAse treatment was efficient to reduce blue Hyaluronan staining**.** Evaluation of the approximate size of Hyaluronan chains by comparison with polymer size marker indicated that adipocytes produced Hyaluronan up to 2000 KD, roughly corresponding to chains formed with more than 5000 sugar units **(Fig 1A)**. HAse efficiency was confirmed by fluorescence imaging with biotinylated Hyaluronan Binding Protein (HABP), which indicated strong cell labelling in untreated permeabilized cells or in cells treated with heat inactivated HAse, drastically reduced following addition of the active HAse enzyme **(Fig 1B)**.

We first examined whether extracellular Hyaluronan degradation might modify the metabolite landscape of adipose tissue microenvironment. We found that Threose was the only differentially produced metabolite following HAse exposure **(Fig 1C)**. Regarding tissue transcriptional profile, RNA-Seq revealed broad gene expression changes following extracellular HAse removal, explored by GSEA **(Fig 1D)**. Not surprisingly, GSEA pointed to gene sets related to inflammation among enriched pathways, which might be the result of activation of adipose tissue immune cells by HAse treatment. Hyaluronidase treatment also induced down-regulation of genes related to adipogenesis and fatty acid metabolism, suggesting that formation of new adipocytes might be a process affected by extracellular hyaluronan removal **(Fig 1E)**.

We next assessed if exogenous hyaluronidase could acutely affect the function of adipocytes. After HAse treatment for 2 days, acute insulin response, a major contributor to lipid storage, evaluated by serine phosphorylation of Akt in the presence of maximal concentrations of insulin was found unaffected **(Suppl Fig 1A),** as well as lipolytic lipid mobilization assessed by glycerol release in response to adrenergic stimulation **(Suppl Fig 1B)**. Thus, no acute effect of HAse was seen on fully mature cultured adipocytes.

Hyaluronidase exposure inhibits adipose differentiation of 3T3-L1 cells

To investigate inhibition of adipose conversion by HAse exposure, 3T3L1 cells were chronically exposed to increasing doses of HAse thoughout the whole differentiation process, starting from confluence (day

0), and including the induction period (from day 0 to day 2) up to day 8. No sign of reduction of cell viability was observed upon HAse exposure (data not shown), but the density of terminally differentiated adipocytes containing refringent lipid droplets was dose-dependently reduced in living cells treated with HAse, compared to untreated controls **(Fig 2A)**. In cells continuously exposed to medium containing the highest HAse concentration (400µg/ml) the staining of lipid droplets with LipidTox at Day 14 was very low compared to untreated controls that differentiated normally **(Fig 2B)**. Drastically reduced lipid accumulation in the presence of native HAse (but not with heat inactivated enzyme) was confirmed by oil red O staining, and could be observed within a time frame of HAse exposure covering the whole differentiation period or the early induction period only **(Fig 2C).**

In line with restricted lipid droplet formation, the expression of differentiation-related genes was reduced in HAse exposed cells, with decreased induction of terminal adipose specific markers including *Glut4, Fasn, Fabp4, Cd36 and Adipoq* **(Fig 2D)**. Among early-induced genes known to acutely respond addition of the differentiation cocktail, *Klf2*, *Klf4*, *Cebpdelta* and *Cepbbeta* mRNA peaked within the 4 hours following induction, with similar amplitude in controls, HAse treated or heat inactivated treated cells **(Fig 2E).** However, 24 hours post induction, a significantly lower level of *Pparg* expression could be detected in HAse treated cells and at 48-hours post-induction, both *Pparg* and *Cebpalpha* mRNA were down-regulated by HAse exposure **(Fig 2E)**. *Cepba* expression remained lower in HAse treated cells throughout the whole differentiation period until day 10 **(Fig 2D)**. To ensure that we did not miss potential HAse-dependent changes in the induction of early genes that respond within the very first hours of differentiation cocktail addition, an additional experiment was performed in which HAse was added 4 hours before the MIX-DEX-INS cocktail. This experiment with HAse pre-treatment confirmed that *Klf2*, *Klf4*, *Cebpb* and *Cebpd* induction patterns were not affected by HAse, and also confirmed the block in *Cebpa* and *Pparg* expression at 24-48 hours post-induction (**Suppl Fig 2A-B**).

We next wanted to investigate if inhibition of adipose differentiation by HAse was restricted to the 3T3L1 cell line or could also be observed in primary adipose progenitors isolated from mice tissues. After collagenase digestion of mice white (epididymal and subcutaneous) or brown (periscapular) adipose fat pads to isolate non lipid-filled preadipocytes contained in the stroma-vascular cell fraction, cells were plated in serum containing medium for 5 days in the presence or absence of exogenous HAse from day 1. *Pparg* mRNA was expressed in primary progenitors from all three adipose tissue locations (epididymal, subcutaneous or scapular) at day 5, except in HAse-exposed cells in which it was almost undetectable **(Suppl Fig 2C)**. *Cebpa* gene expression was also strongly reduced in HAse treated progenitors whatever their tissue origin **(Suppl Fig 2D).** All together, these data demonstrate that the removal of extracellular Hyaluronan has a strong negative impact on adipocyte differentiation, seen not only in an established adipose cell line, but also in mice primary progenitors isolated from mice adipose tissue. Moreover, we show here that co-regulated C/EBPα and PPARγ expression are the targets of HAse-dependent blockade of adipose differentiation. We also observed that Hyaluronan removal from the 3T3L1 cell environment did not affect the expression of other ECM-related genes like collagen 1 mRNA **(Suppl Fig 2E)**. Fibronectin mRNA expression was increased in both HAse and heat inactivated HAse 3T3L1 cells compared to untreated controls **(Suppl Fig 2F)**.

Mechanistic insight into Hyaluronidase-mediated inhibition of adipose differentiation

A number of studies have established inflammation among inhibitors of adipogenesis, and hyaluronan status is closely linked to the tissue microenvironment inflammatory state. Especially it was reported in

different tissue contexts that the presence of short Hyaluronan fragments associated with a pro-inflammatory condition (21). Thus, a simple explanation for adipogenesis blockade by extracellular Hyaluronan degradation could rely on activated inflammatory cytokine production, which might secondarily prevent fat cell conversion. However, we could detect no change in cytokine expression in HAse-treated cells compared to untreated controls or cells treated with heat inactivated enzyme. Indeed, *Tgfb1, Tgfb*3 and *Spp1* mRNAs which encode cytokines with the highest expression in early differentiating cells **(Fig 3A)**, and *Ccl2*, *Spp1* and *Tgfb1* which are the most expressed in terminally differentiated adipocytes **(Fig 3B)** were not affected by HAse exposure. Thus, although assessed solely at the mRNA level, inflammation is unlikely the cause of adipogenesis blockade by extracellular hyaluronan removal.

We next examined the possibility that threose production which was identified in our metabolomic screen following exposure of adipose samples to HAse might inhibit adipose cell differentiation **(Fig 1C)**. Indeed, threose is a four-carbon sugar that can be derived from Hyaluronan degradation following the release of glucoronic acid units further metabolized into ascorbic acid **(Fig 3C).** To test the potential role of threose, 3T3L1 cells were grown to differentiate in the presence of increasing concentrations of the sugar. We observed that threose was not able to mimic the inhibitory effect of HAse, as it did not affect the expression of terminal differentiation gene markers like *Cebpa*, *Fasn*, *Fabp4* and *Adipoq* **(Fig 3D)**. Thus HAse-dependant inhibition of adipogenesis is unlikely mediated by the liberation of threose subsequent to Hyaluronan chains degradation.

Because Hyaluronan is an active osmotic regulator able to bind large amount of water molecules, we reasoned that HAse-mediated inhibition of adipose differentiation could be driven by changes in osmolarity. Indeed, culture medium osmolarity oscillated after HAse incubation for 2-days, which is the time laps between medium changes **(Fig 3E)**. Relative to cells maintained in heat inactivated HAse containing medium, osmotic pressure decreased with HAse exposure (approx. 20mosm reduction). On the contrary, positive changes in osmotic pressure could be induced within the same time frame by exposing cells to 1% mannitol-supplemented media. Noteworthy, mannitol addition in combination with HAse was able to maintain stable medium osmolarity between medium changes, but this combination was inefficient to recover *Cebpa* and *Pparg* gene expression to the levels seen in controls **(Fig 3F)**. Moreover, terminal adipocyte markers *Fasn, Glut4, Adipoq*, and *Cd36* mRNA remained low in the presence of HAse and mannitol, similar to HAse alone **(Fig 3G)**, indicating that preventing the drop in medium osmolarity induced by HAse cannot able to rescue cell differentiation.

In our search for mechanistic insights, we noticed that “Wnt beta catenin signaling”, and “Hedgehog signaling”, well known anti-adipogenic pathways pointed out from GSEA of HAse-treated adipose tissue **(Fig 1D)**. Wnt pathway activation is a strong repressor of fat cell conversion, and down-regulation of endogenous Wnt ligands is necessary for 3T3L1 adipocyte differentiation, whereas overexpression is able to suppress adipose conversion (22). Thus, we examined HAse impact on time-dependent expression of Wnt6 and Wnt10b mRNAs encoding the two main 3T3L1 Wnt endogenous ligands **(Fig 4A-B)**. Wnt6 mRNA declined as early as 2 hours post-induction, whereas Wnt10b mRNA responded more slowly. Surprisingly, at the level of mRNA, low expression of Wnt6 and Wnt10b was observed in cells exposed to HAse compared to controls, against the possibility that HAse exposure could inhibit adipogenesis through activation of Wnt signalling.

An early event that we could detect within hours following the induction of 3T3L1 differentiation in the presence of HAse was a transitory 3-fold stimulation of Cd44 expression, a known receptor for extracellular Hyaluronan and a complex signaling molecule **(Fig 4C)**. The expression of another cell surface Hyaluronan interacting protein, i.e Hyaluronan mediated mobility Receptor (Hmmr) was unaffected (not shown). We also noticed simultaneous upregulation of Matrix Gla protein (Mgp) mRNA expression in cells exposed to HAse **(Fig 4D)**, which encodes a calcium binding protein recently indentified as a stemness marker in (23)**.** These observations point to a Cd44 receptor/calcium-dependent pathway in HAse inhibition of early adipogenesis. We also noticed changes the cilia dynamics in cells differentiated in the presence of HAse **(Fig 4E)**. Linked to the cell primary cilium functioning as an antenna in the sensing of extracellular milieu, it was previously reported that differentiating adipocytes disassemble their cilia during maturation *in vivo* and *in vitro* (24)(25). We found a differentiation-dependent decline in the proportion of ciliated cells in control conditions, which was not observed in HAse exposed cultures **(Fig 4F)**. In addition, cilia length distributions were right-shifted in HAse treated cells compared to controls **(Fig 4G),** with cilia length peaking in the 2-4 micron class in control cells, versus 4-6 micron in HAse exposed cells. Thus, extracellular Hyaluronan removal is associated with conservation of longer cilia over time, a finding that suggests altered cilia disassembly with potential to explain the differentiation blockade. This highlights a novel mechanism by which extracellular Hyaluronan might impact fat cell differentiation, linked to modulation of ciliogenesis, especially regulation of cilium length and disassembly.

To confirm cilia alteration in human adipose tissue upon HAse exposure, we merged the lists of differentially regulated genes (DEGs) from RNA Seq with that established in the Ciliacarta compendium (26) which defined a predictive score for ciliary function according to integrated analysis of genomic, proteomic and evolutionary data. Among 9319 HAse-regulated DEGs (significance threshold <0.05), we retrieved 105 genes with a cilia score higher than 1, meaning a twice more likelihood to be ciliary than non-ciliary (**Fig 4H**). Four intraflagellar transport genes (IFT 57, 88, 46 and 122) and Arl13B, among the highest predicted cilia score were also found in DEGs, as well as two BBS genes (BBS4 and BBS12), known to be responsible of Bardet-Biedel ciliopaties when mutated **(Suppl Table 1)**. These data on human adipose tissue are in line with our morphological analysis in 3T3-L1 preadipocytes that HAse exposure associates with cilia dysregulation.

Discussion

Little is known on the importance of hyaluronan and proteoglycan metabolism in adipose tissue biology (27). Back in the 90s, using the 3T3L1 cell line as a model for developing fat cells, it was reported that hyaluronan and proteoglycans synthetic capacity was low in adipocytes compared to fibroblastic preadipocytes (28), a feature that is in good accordance with the high capacity for matrix production of adipose tissue progenitors. Moreover, it was reported that 3T3L1 preadipocytes rapidly responded (within 24hours) adipogenic induction by a peak in the expression of Hyaluronan synthetic enzymes, mainly HASynthase 2 and 3 (29). These early observations suggested that Hyaluronan impact might be exerted preferentially in the early steps of adipose conversion. Indeed, *in vitro* limitation of Hyaluronan extracellular deposition by 4MU-induced inhibition of Hyaluronan synthesis had similar anti-adipogenic effects than extracellular degradation with exogenous Hyaluronidase exposure (4). Our findings are also in line with the report that Hyaluronidase infusion *in vivo* could block the process of reactive

adipogenesis that relates to the development of fat tissue formation around injured colon or skin (5). We show here that adipogenic blockade by extracellular Hyaluronan removal appears a general process not limited to the 3T3L1 model which also operates in cultured primary progenitors isolated from mouse adipose tissue. We also document here that the anti-adipogenic effects of extracellular hyaluronan degradation converge in the early induction of the two main transcriptional regulators of adipogenesis i.e. C/EBPalpha and PPARgamma. Of note, the report by Park and colleagues that 3T3L1 cell exposure to a milieu enriched in Hyaluronan (in the form of small-sized Hyaluronan enzymatic fragments) also repressed adipose differentiation seems counterintuitive (30). However, in the latter study, short-chain Hyaluronan was obtained by treating polymers with bacterial HAse followed by separation of hydrolytic fragments by filtration, and it cannot be excluded that contaminating HAse enzyme could be responsible for anti-adipogenic effect.

Our search for the mechanisms driving the anti-adipogenic action of Hyaluronan removal led us to exclude several potential candidates. Firstly, we found that mitigating osmotic changes associated with cell exposure to HAse (by buffering medium osmolarity with mannitol) was inefficient to rescue cell differentiation, making unlikely changes in osmotic pressure as a driving force. Secondly, we could also eliminate the possibility that Hyaluronan degradation could generate a sugar metabolite with potential anti-adipogenic properties (such as Threose, a single hit in metabolomics screen), or cause pro-inflammatory cell activation, as observed in other cell types (21). Finally, we found no evidence that HAse exposure could activate the production of endogenous Wnt ligands, those downregulation is a required step in 3T3L1 cells adipogenesis (22).

As an early response to extracellular HA removal, our study identifies Cd44, induced within hours of HAse exposure. Cd44 is not only a cellular binding receptor with high affinity for extracellular Hyaluronan, but also an important molecule in the regulation of adipose progenitors. It is referred to as a cell surface marker indicative of an early state in adipose commitment (31), and is expressed in proliferating adipose progenitors targeted to tissue sites of adipocyte clearance (32). More generally, Cd44 is considered a molecule that favors mesenchymal cell stemness (33). It is possible that signaling pathways downstream of Cd44 might mediate the anti-adipogenic response to Hyaluronan removal. In this context, A Cd44-dependent endocytic pathway linked to iron endocytosis has recently been described (34), but we did not observed dependency of iron status on 3T3L1 cell response to Hyaluronan removal (data not shown).

An original finding in our study is that anti-adipogenic Hyaluronan removal associates with primary cilia alterations. We report that HAse exposure increased cilia length, and raised the proportion of cells that remain ciliated over differentiation time course. In line with cilia behaving as protuberances for the sensing of extracellular environment, recent data indicate that nutritional regulators such as omega-3 fatty acids (24) or glutamine (35) exert regulatory functions by signaling through this organelle. This is the first study to suggest a link between primary cilium and extracellular Hyaluronan. Interestingly, we observed common cilia length elongation in preadipocytes and in immortalized mouse embryonic fibroblasts upon hyaluronidase exposure (data not shown) suggesting that cilia length is sensitive to extracellular hyaluronan, independent of cell fate determination. In the specific context of adipose differentiation, since we found upregulation of cilia numbers and length with Hyaluronan removal, it is

likely that extracellular Hyaluronan impacts the disassembly of the cilia antenna, a process required for fat cell differentiation to proceed (25). Whether such a regulation involves Cd44 signaling remains an open question. Although not directly related to adipogenesis, a recent study suggests that the primary cilium controls osteopontin-dependent Cd44 signaling in migrating mesenchymal cells (36). Noteworthy, serum concentrations of Hyaluronan rise with high fat feeding in mice models of obesity (37), and increased circulating Hyaluronan also associated with type 2 diabetes and liver cirrhosis (38) (39). Thus, more attention would be required on adipose tissue Hyaluronan fluctuation across BMI classes in human subjects.

Limitations of the study:

Our study points to a new link between hyaluronan-regulated adipocyte differentiation and primary cilia dynamics. However, it cannot be established from the present data if cilia alterations are directly induced by hyaluronan removal or if they are secondary to inhibition of differentiation by HAse. In other words, there is no direct evidence that the modification in cilium size is the cause of the decrease in adipocyte differentiation or its consequence. Also, although we demonstrated that changes in osmolarity cannot explain anti-adipogenic effects of hyaluronan removal, we did not address the question of potential alterations in the physical properties (elasticity, stiffness) of the extracellular matrix lacking hyaluronan, that might impact adipose differentiation. Finally, we did not examine if hyaluronidase-mediated changes are reversible i.e. if reintroduction of exogenous hyaluronan can overcome differentiation blockade.

Reference list

1. Pellegrinelli V, Heuvingh J, Du Roure O, Rouault C, Devulder A, Klein C, et al. Human adipocyte function is impacted by mechanical cues. J Pathol. 2014;233(2):183–95.
2. Khan T, Muise ES, Iyengar P, Wang Z V., Chandalia M, Abate N, et al. Metabolic Dysregulation and Adipose Tissue Fibrosis: Role of Collagen VI. Mol Cell Biol. 2009;29(6):1575–91.
3. Zhu Y, Li N, Huang M, Bartels M, Dogné S, Zhao S, et al. Adipose tissue hyaluronan production improves systemic glucose homeostasis and primes adipocytes for CL 316,243-stimulated lipolysis. Nat Commun. 2021;12(1).
4. Ji E, Jung MY, Park JH, Kim S, Seo CR, Park KW, et al. Inhibition of adipogenesis in 3T3-L1 cells and suppression of abdominal fat accumulation in high-fat diet-feeding C57BL/6J mice after downregulation of hyaluronic acid. Int J Obes (Lond). 2014 Aug;38(8):1035–43.
5. Dokoshi T, Zhang LJ, Nakatsuji T, Adase CA, Sanford JA, Paladini RD, et al. Hyaluronidase inhibits reactive adipogenesis and inflammation of colon and skin. JCI insight. 2018;3(21):1–12.
6. Marcelin G, Silveira ALM, Martins LB, Ferreira AVM, Clément K. Deciphering the cellular interplays underlying obesityinduced adipose tissue fibrosis. J Clin Invest. 2019;129(10):4032–40.
7. Divoux A, Clément K. Architecture and the extracellular matrix: The still unappreciated components of the adipose tissue. Obes Rev. 2011;12(501).
8. Lassen PB, Charlotte F, Liu Y, Bedossa P, Le Naour G, Tordjman J, et al. The fat score, a fibrosis score of adipose tissue: Predicting weight-loss outcome after gastric bypass. J Clin Endocrinol Metab. 2017;102(7):2443–53.
9. Sun K, Tordjman J, Clément K, Scherer PE. Fibrosis and adipose tissue dysfunction. Cell Metab.

2013;18(4):470–7.

10. Divoux A, Tordjman J, Lacasa D, Veyrie N, Hugol D, Aissat A, et al. Fibrosis in Human Adipose Tissue : Composition , Distribution , and Link With Lipid Metabolism and Fat. Diabetes. 2010;59:2817–25.

11. Marcelin G, Ferreira A, Liu Y, Atlan M, Aron-Wisnewsky J, Pelloux V, et al. A PDGFRα-Mediated Switch toward CD9highAdipocyte Progenitors Controls Obesity-Induced Adipose Tissue Fibrosis. Cell Metab. 2017;25(3):673–85.

12. Hepler C, Shan B, Zhang Q, Henry GH, Shao M, Vishvanath L, et al. Identification of functionally distinct fibro-inflammatory and adipogenic stromal subpopulations in visceral adipose tissue of adult mice. Elife. 2018;7:1–36.

13. Lee MJ. Transforming growth factor beta superfamily regulation of adipose tissue biology in obesity. Biochim Biophys Acta - Mol Basis Dis. 2018;1864(4):1160–71.

14. Lecoutre S, Merabtene F, El Hachem E-J, Gamblin C, Rouault C, Sokolovska N, et al. Beta-hydroxybutyrate dampens adipose progenitors' profibrotic activation through canonical Tgfβ signaling and non-canonical ZFP36-dependent mechanisms. Mol Metab. 2022 Jul;61(May):101512.

15. Madsen DH, Leonard D, Masedunskas A, Moyer A, Jürgensen HJ, Peters DE, et al. M2-like macrophages are responsible for collagen degradation through a mannose receptor-mediated pathway. J Cell Biol. 2013;202(6):951–66.

16. Miniewska K, Godzien J, Mojsak P, Maliszewska K, Kretowski A, Ciborowski M. Mass spectrometry-based determination of lipids and small molecules composing adipose tissue with a focus on brown adipose tissue. J Pharm Biomed Anal. 2020;191:113623.

17. Mojsak P, Maliszewska K, Klimaszewska P, Miniewska K, Godzien J, Sieminska J, et al. Optimization of a GC-MS method for the profiling of microbiota-dependent metabolites in blood samples: An application to type 2 diabetes and prediabetes. Front Mol Biosci. 2022 Sep;9.

18. Love MI, Huber W, Anders S. Moderated estimation of fold change and dispersion for RNA-seq data with DESeq2. Genome Biol. 2014 Dec;15(12):550.

19. Blouin CM, Le Lay S, Lasnier F, Dugail I, Hajduch E. Regulated association of caveolins to lipid droplets during differentiation of 3T3-L1 adipocytes. Biochem Biophys Res Commun. 2008;376(2):331–5.

20. Subramanian A, Tamayo P, Mootha VK, Mukherjee S, Ebert BL, Gillette MA, et al. Gene set enrichment analysis: A knowledge-based approach for interpreting genome-wide expression profiles. Proc Natl Acad Sci U S A. 2005;102(43):15545–50.

21. Campo GM, Avenoso A, Campo S, D'Ascola A, Nastasi G, Calatroni A. Small hyaluronan oligosaccharides induce inflammation by engaging both toll-like-4 and CD44 receptors in human chondrocytes. Biochem Pharmacol. 2010 Aug;80(4):480–90.

22. Ross SE, Hemati N, Longo KA, Bennett CN, Lucas PC, Erickson RL, et al. Inhibition of adipogenesis by Wnt signaling. Science (80-). 2000;289(5481):950–3.

23. Yang Loureiro Z, Joyce S, DeSouza T, Solivan-Rivera J, Desai A, Skritakis P, et al. Wnt signaling preserves progenitor cell multipotency during adipose tissue development. Nat Metab.

2023;5(6):1014–28.

24. Hilgendorf KI, Johnson CT, Mezger A, Rice SL, Norris AM, Demeter J, et al. Omega-3 Fatty Acids Activate Ciliary FFAR4 to Control Adipogenesis. Cell. 2019;179(6):1289-1305.e21.

25. Forcioli-Conti N, Lacas-Gervais S, Dani C, Peraldi P. The primary cilium undergoes dynamic size modifications during adipocyte differentiation of human adipose stem cells. Biochem Biophys Res Commun. 2015;458(1):117–22.

26. Van Dam TJP, Kennedy J, van der Lee R, de Vrieze E, Wunderlich KA, Rix S, et al. Ciliacarta: An integrated and validated compendium of ciliary genes. Vol. 14, PLoS ONE. 2019. 1–32 p.

27. Drygalski K, Lecoutre S, Clément K, Dugail I. Hyaluronan in Adipose Tissue, Metabolic Inflammation, and Diabetes: Innocent Bystander or Guilty Party? Diabetes. 2023;72(2):159–69.

28. Musil KJ, Malmström A, Donnér J. Alteration of proteoglycan metabolism during the differentiation of 3T3-L1 fibroblasts into adipocytes. J Cell Biol. 1991 Aug;114(4):821–6.

29. Allingham PG, Brownlee GR, Harper GS, Pho M, Nilsson SK, Brown TJ. Gene expression, synthesis and degradation of hyaluronan during differentiation of 3T3-L1 adipocytes. Arch Biochem Biophys. 2006 Aug;452(1):83–91.

30. Park B-G, Lee CW, Park JW, Cui Y, Park Y-S, Shin W-S. Enzymatic fragments of hyaluronan inhibit adipocyte differentiation in 3T3-L1 pre-adipocytes. Biochem Biophys Res Commun. 2015 Nov;467(4):623–8.

31. Chen M, Kim S, Li L, Chattopadhyay S, Rando TA, Feldman BJ. Identification of an adipose tissue-resident pro-preadipocyte population. Cell Rep. 2023;42(5):112440.

32. Lee Y-H, Petkova AP, Granneman JG. Identification of an adipogenic niche for adipose tissue remodeling and restoration. Cell Metab. 2013 Sep;18(3):355–67.

33. Wong TY, Chang CH, Yu CH, Huang LLH. Hyaluronan keeps mesenchymal stem cells quiescent and maintains the differentiation potential over time. Aging Cell. 2017;16(3):451–60.

34. Müller S, Sindikubwabo F, Cañeque T, Lafon A, Versini A, Lombard B, et al. CD44 regulates epigenetic plasticity by mediating iron endocytosis. Nat Chem. 2020;12(10):929–38.

35. Steidl ME, Nigro EA, Nielsen AK, Pagliarini R, Cassina L, Lampis M, et al. Primary cilia sense glutamine availability and respond via asparagine synthetase. Nat Metab. 2023;

36. Lee MN, Song JH, Oh SH, Tham NT, Kim JW, Yang JW, et al. The primary cilium directs osteopontin-induced migration of mesenchymal stem cells by regulating CD44 signaling and Cdc42 activation. Stem Cell Res. 2020;45(March):101799.

37. Kang L, Lantier L, Kennedy A, Bonner JS, Mayes WH, Bracy DP, et al. Hyaluronan accumulates with high-fat feeding and contributes to insulin resistance. Diabetes. 2013;62(6):1888–96.

38. Nagy N, Sunkari VG, Kaber G, Hasbun S, Lam DN, Speake C, et al. Hyaluronan levels are increased systemically in human type 2 but not type 1 diabetes independently of glycemic control. Matrix Biol. 2019;80:46–58.

39. Parés A, Deulofeu R, Giménez A, Caballería L, Bruguera M, Caballería J, et al. Serum hyaluronate reflects hepatic fibrogenesis in alcoholic liver disease and is useful as a marker of fibrosis.

Hepatology. 1996;24(6):1399–403.

Figure legends

Figure 1 : Impact of exogenous HAse exposure

A : Confluent (Day 0) 3T3-L1 cells were fed 3 times a week with fresh medium containing vehicle or 400µg/ml native or heat inactivated HAse. At indicated times, cell medium was collected for HA extraction, and extracted material was run onto 0.5% agarose gels followed by revelation with "Stains All" reagent (HA in blue, nucleic acids in purple. A typical experiment is shown.
B: Confluent 3T3-L1 cells were incubated with vehicle or 400µg/ml native or heat inactivated HAse for 5 days before cell layer fixation with paraformaldehyde and incubation with biotinylated HABP (1:200, SigmaAldrich, France) at 4 ^{o}C overnight followed by incubation with fluorescent streptavidin (1:1000, Vector Laboratories, France). Subsequently cells were visualized with confocal microscope (Olympus FV1200, Germany). Representative images are shown.
C: Analysis of differentially present metabolites in adipose tissue samples with or without 400µg/ml HAse treatment for 24h. Data were analysed from 3-5 different slices prepared from subcutaneous adipose tissue samples obtained from 3 individual lean male subjects. Volcano plot highlights Threose as an overproduced metabolite after extracellular Hyaluronan removal.
D: GSEA analysis from RNAseq performed on subcutaneous adipose tissue maintained in serum containing culture medium in the presence or absence of Hyaluronidase for 24 h. Tissue samples were obtained from 3 healthy subjects assayed in 4 biological replicates. Normalised enrichment scores for listed gene sets from the Hallmark collection are shown. The size of points is proportional to FDR values from 0.05.
E: The distribution of « adipogenesis » gene set in the HAse-treated adipose tissue samples (B) versus non HAse treated (REST).

Figure 2: HAse inhibits differentiation of 3T3L1 adipocytes

A : Phase contrast imaging of differentiated 3T3L1 cells maintained in standard condition (0) or in HAse containing medium at indicated concentrations. HAse was added from confluence, including the induction period with MIX/DEX/INS until day 8. Highly refringent cells are laden with lipid droplets. A representative experiment is shown.
B: Fluorescent imaging of terminally differentiated cells showing nuclei (Dapi) or lipid droplets (LipidTOX) in cells continuously maintained in a medium containing HAse or not.
C: Oil red O staining of neutral lipids in culture dishes at day 8 post induction. Cells received treatment as indicated from Day 0 to Day 8 (left part) or from Day 0 to Day 2 (right part).
D: Time course of adipose specific gene expression during differentiation of 3T3-L1 cells treated from Day 0 with native HAse (Blue) or heat inactivated enzyme (red). mRNAs were quantified by RT-QPCR and normalized to ribosomal 18S RNA. Relative expression values are means +/- sem from three independent experiments. * indicates significant difference between groups by Student's t test ($p<0.05$).
E: Expression of early differentiation marker genes during the first 2 days following induction with MIX-DEX-INS cocktail, added alone (black) or with native HAse (blue) or with heat inactivated enzyme (red).

Indicated mRNAs were assessed by RT-QPCR. Values are means +/- sem from three independent experiments. Significant differences ($p<0.05$) by Student's t test are indicated with brackets.

Figure 3 : Mechanistic insight into HAse mediated inhibition of adipocyte differentiation.

A-B: Inflammatory cytokines mRNA expression in 3T3L1 preadipocytes at Day 2 (A) or in fully differentiated adipocytes at Day 10 (B). Treatment with HAse or hiHAse is applied at day 0 onwards. Bars are mean values +/- sem of 3 independent experiments.
C: Glucuronic acid generated after hyaluronan polymer degradation by HAse action can produce Threose. Most reactions indicated as dashed lines are non-enzymatic.
D: Threose is not able to mimic HAse-mediated inhibition of adipose differentiation: 3T3L1 cells were allow to differentiate in standard conditions (Ctrl), with 0.4mg/ml native HAse or heat inactivated (hiHAse), or in the presence of increasing Threose concentrations (from 0.1 to 5 mM). After 10 days, total RNA was extracted to measure gene expression by RT-QPCR. Bars represent mean values +/- sem from 2 independent experiments.
E: Changes in culture medium osmolarity after 2 days incubation with differentiating cells. Each point is a delta value obtained between two medium changes from Day 2 to Day 10.
F-G: Adipocyte mRNA expression is not restored in cells treated with a combination of HAse and mannitol. After 10 days, total RNA was extracted for RT-QPCR. Bars represent mean values +/- sem from 2 independent experiments. Brackets indicate significant differences by student's t test ($p<0.05$)

Figure 4: HAse-mediated inhibition of differentiation is Cd44-dependent and linked to defective cilia disassembly.

A-B: Time course of endogenous Wnt mRNA expression in early differentiation. Pretreatment with HAse, hiHAse or vehicle was performed 4 hours before addition of the differentiation cocktail. Values are means +/- sem from three independent experiments.
C-D: Time course of *Cd44* and *Mgp* mRNA by RT-QPCR in early differentiation. Cells were maintained as in A. Mean values +/-sem were obtained from 3 independent experiments.
E: Primary cilia visualization after staining with ARL13 antibody (green) and Dapi (blue). Representative images are shown.
F: Quantification of the percentage of cells with a cilia during differentiation of control and HAse-treated cultures. The total number of cells analyzed in each condition is shown in parentheses.
G: Cilia length measurements. ImageJ software was used to measure each cilia individually after processing of stacks with Z project. Frequency distributions were obtained for 2µm interval classes. The legend indicates differentiation time, cell condition and the total number of cilia processed in each condition (in parentheses). H: Schematic representation of HAse-mediated gene expression changes in human adipose tissue.

Declaration of interests

☒The authors declare that they have no known competing financial interests or personal relationships that could have appeared to influence the work reported in this paper.

☐The authors declare the following financial interests/personal relationships which may be considered as potential competing interests:

Graphical abstract

Highlights

Extracellular Hyaluronan removal impacts human adipose tissue gene expression

Hyaluronidase exposure inhibits adipose differentiation in 3T3L1 cells and primary progenitors

Hyaluronidase-mediated inhibition of adipose differentiation is not linked to changes in osmolarity, inflammation or activation of Wnt signalling.

Hyaluronan removal promotes primary cilia elongation and prevents differentiation-dependent cilia number decline.

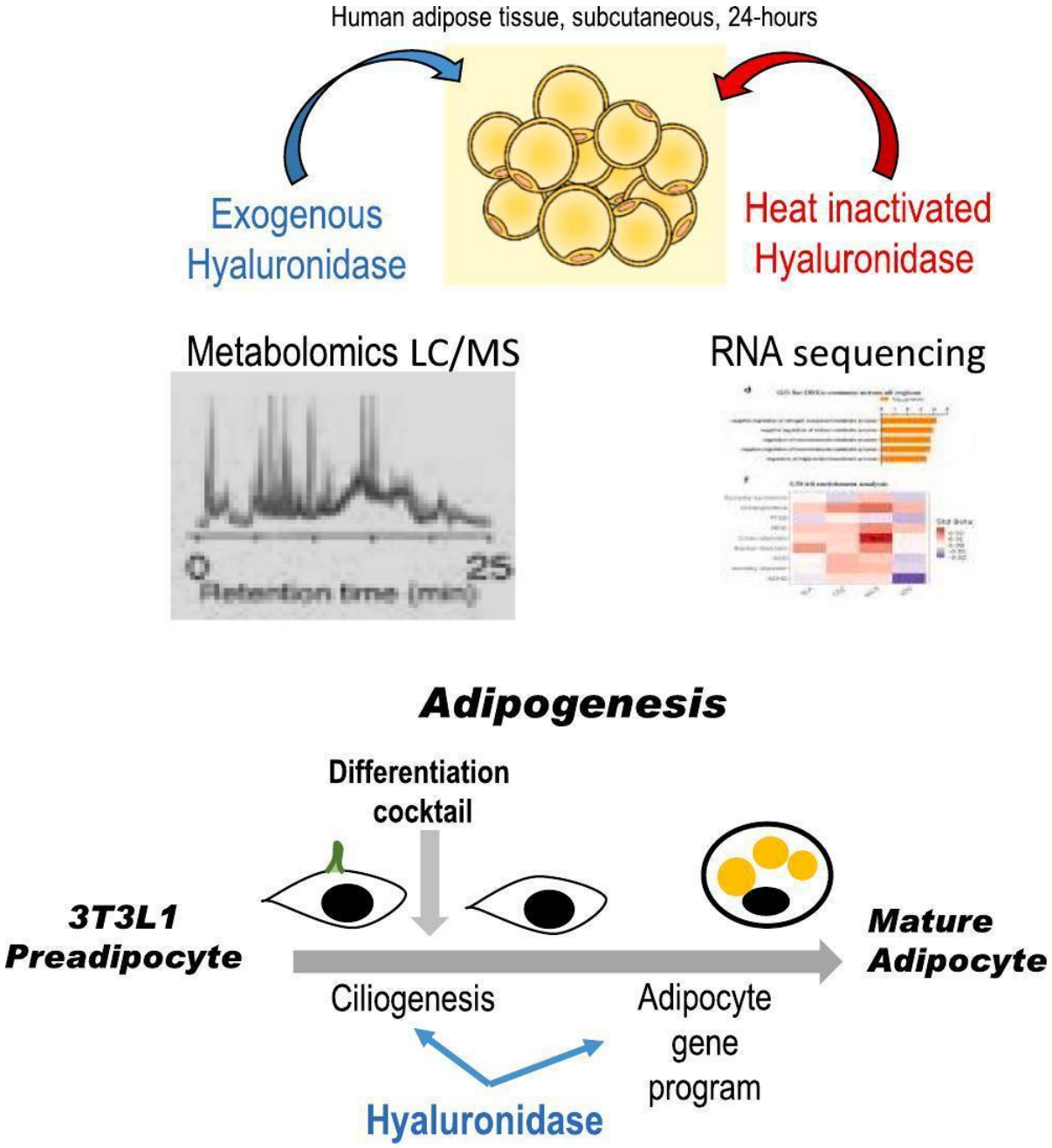

Graphics Abstract

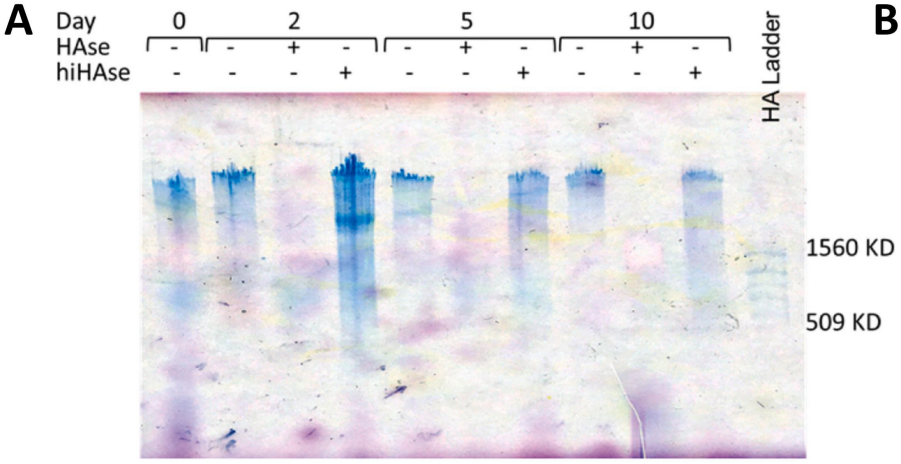
A
Day
0
2
5
10
HAse
hiHAse
HA Ladder
1560 KD
509 KD

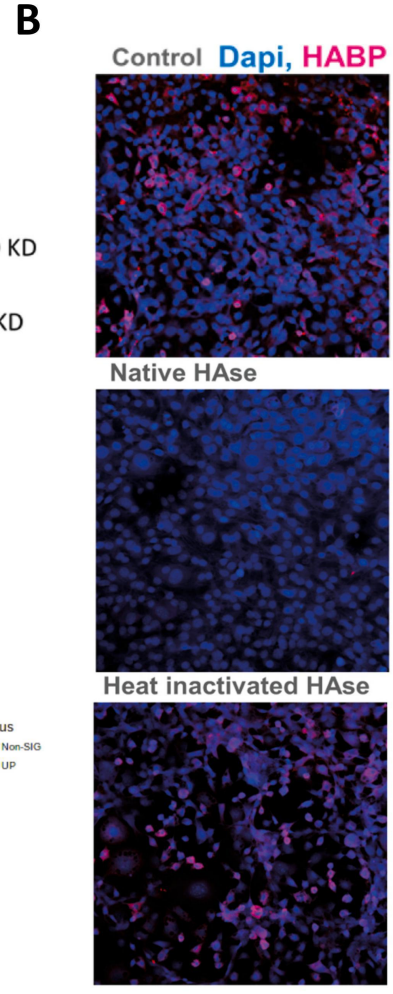
B
Control
Dapi, HABP
Native HAse
Heat inactivated HAse

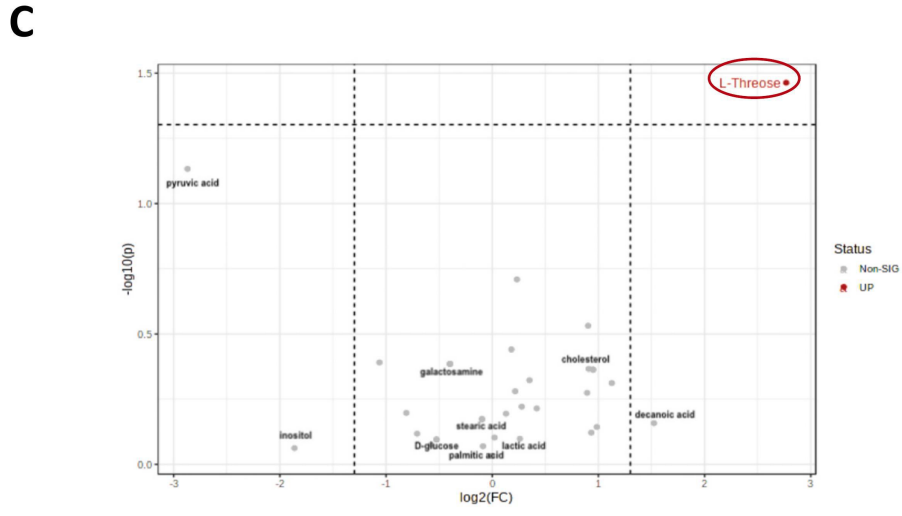
C
L-Threose
pyruvic acid
inositol
galactosamine
cholesterol
decanoic acid
stearic acid
D-glucose
lactic acid
palmitic acid
-log10(p)
log2(FC)
Status
Non-SIG
UP

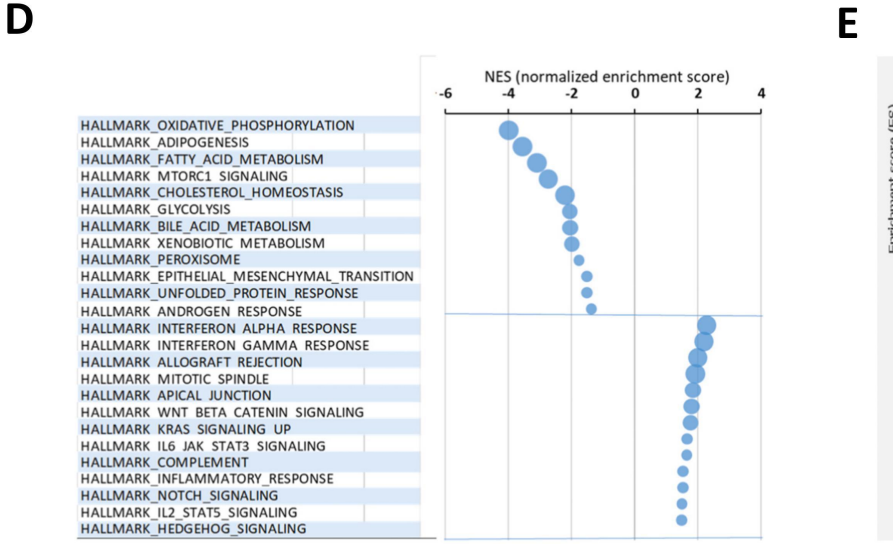
D
NES (normalized enrichment score)
HALLMARK_OXIDATIVE_PHOSPHORYLATION
HALLMARK_ADIPOGENESIS
HALLMARK_FATTY_ACID_METABOLISM
HALLMARK_MTORC1_SIGNALING
HALLMARK_CHOLESTEROL_HOMEOSTASIS
HALLMARK_GLYCOLYSIS
HALLMARK_BILE_ACID_METABOLISM
HALLMARK_XENOBIOTIC_METABOLISM
HALLMARK_PEROXISOME
HALLMARK_EPITHELIAL_MESENCHYMAL_TRANSITION
HALLMARK_UNFOLDED_PROTEIN_RESPONSE
HALLMARK_ANDROGEN_RESPONSE
HALLMARK_INTERFERON_ALPHA_RESPONSE
HALLMARK_INTERFERON_GAMMA_RESPONSE
HALLMARK_ALLOGRAFT_REJECTION
HALLMARK_MITOTIC_SPINDLE
HALLMARK_APICAL_JUNCTION
HALLMARK_WNT_BETA_CATENIN_SIGNALING
HALLMARK_KRAS_SIGNALING_UP
HALLMARK_IL6_JAK_STAT3_SIGNALING
HALLMARK_COMPLEMENT
HALLMARK_INFLAMMATORY_RESPONSE
HALLMARK_NOTCH_SIGNALING
HALLMARK_IL2_STAT5_SIGNALING
HALLMARK_HEDGEHOG_SIGNALING

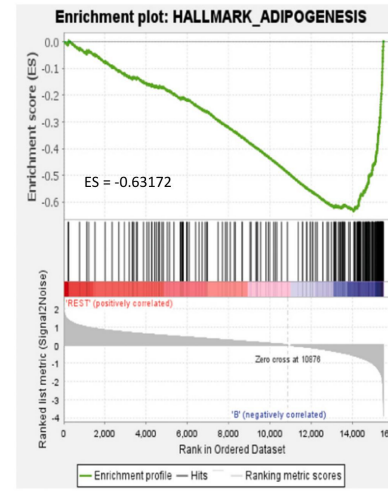
E
Enrichment plot: HALLMARK_ADIPOGENESIS
Enrichment score (ES)
ES = -0.63172
'REST' (positively correlated)
Zero cross at 10676
'B' (negatively correlated)
Ranked list metric (Signal2Noise)
Rank in Ordered Dataset
Enrichment profile
Hits
Ranking metric scores

Figure 1

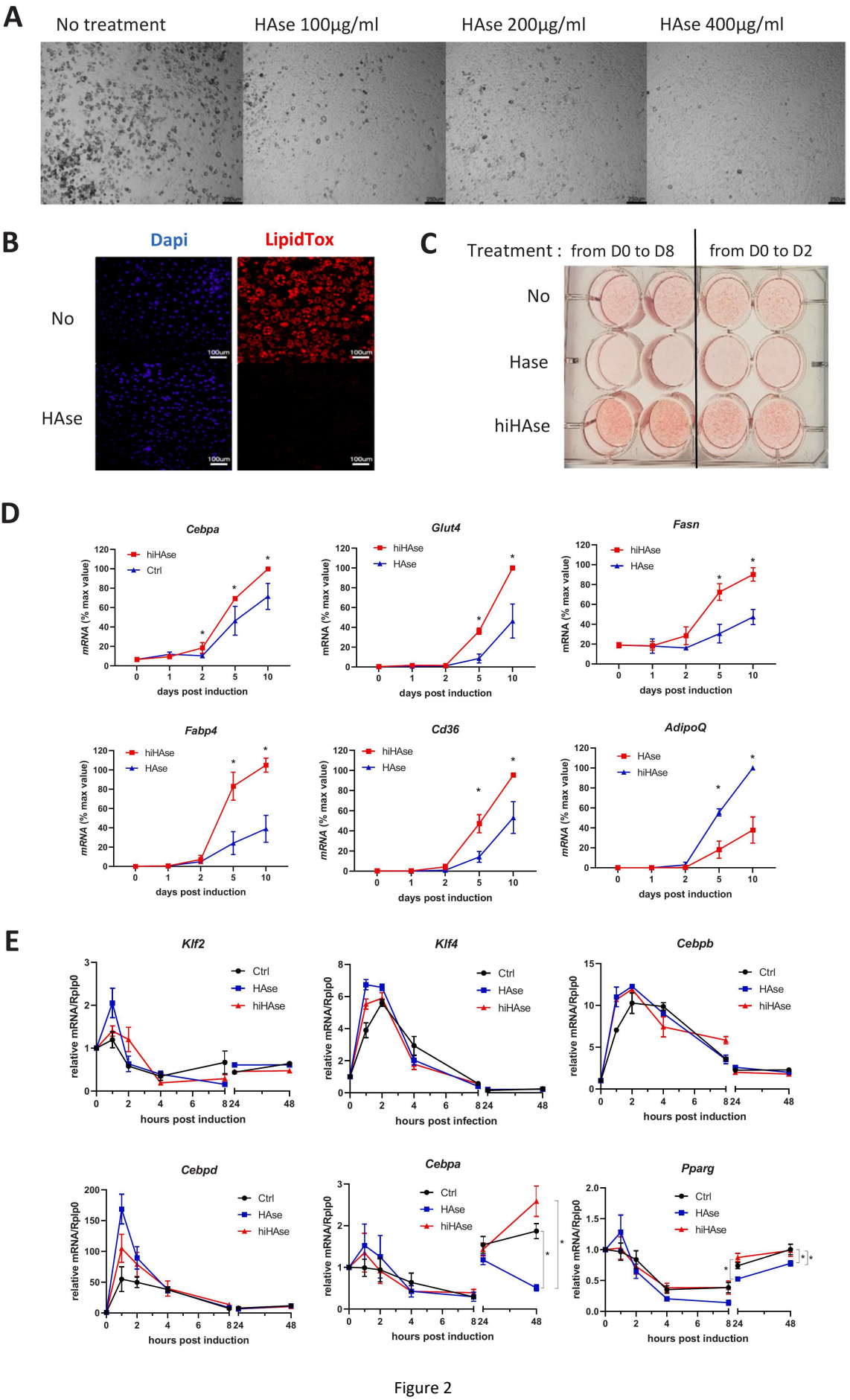
A
No treatment
HAse 100µg/ml
HAse 200µg/ml
HAse 400µg/ml
B
Dapi
LipidTox
No
HAse
100um
C
Treatment : from D0 to D8
from D0 to D2
No
Hase
hiHAse
D
Cebpa
Glut4
Fasn
Fabp4
Cd36
AdipoQ
hiHAse
HAse
Ctrl
mRNA (% max value)
days post induction
E
Klf2
Klf4
Cebpb
Cebpd
Cebpa
Pparg
Ctrl
HAse
hiHAse
relative mRNA/Rplp0
hours post induction
hours post infection

Figure 2

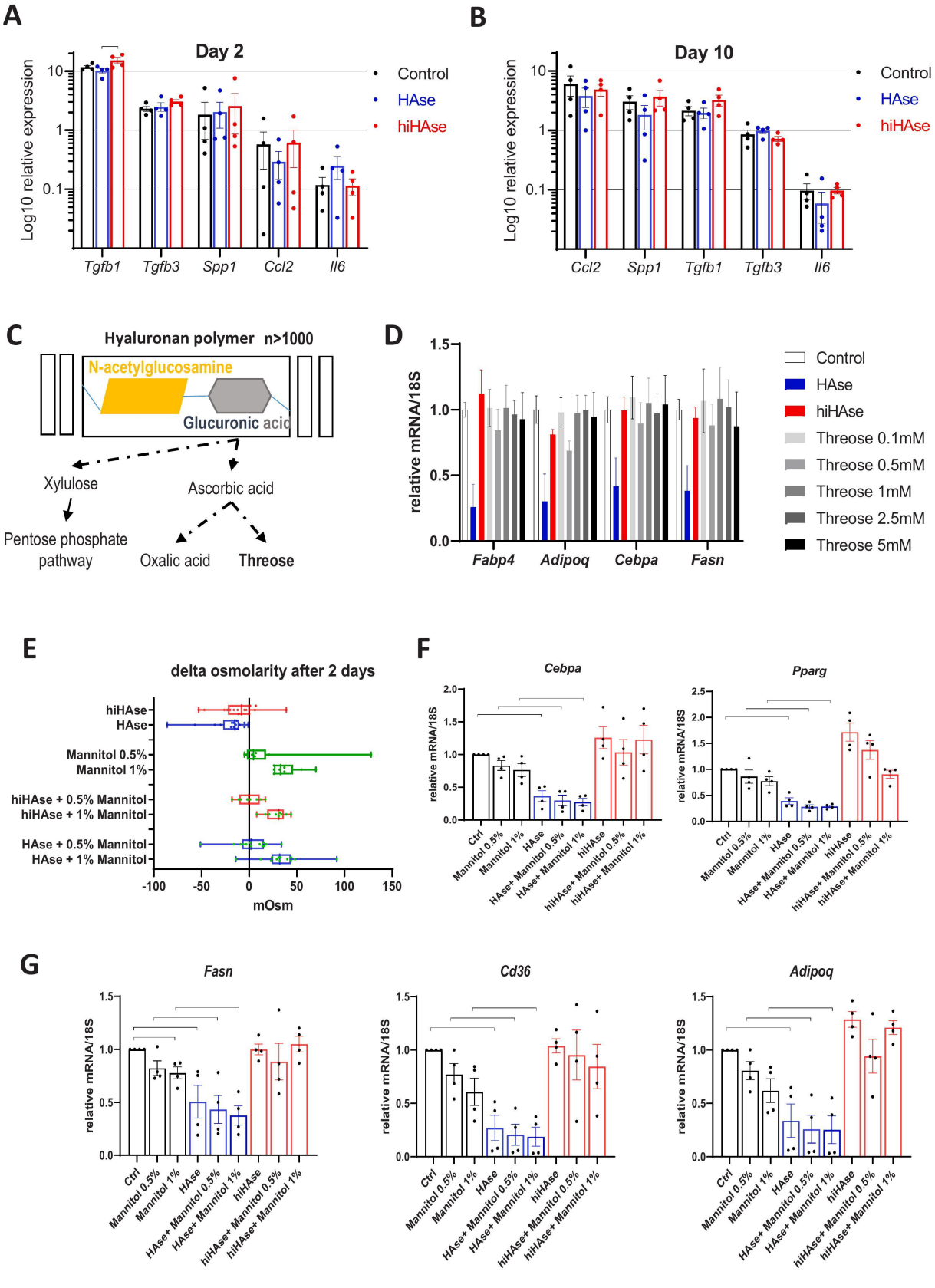
A
Day 2
Log10 relative expression
Control
HAse
hiHAse
Tgfb1
Tgfb3
Spp1
Ccl2
Il6
B
Day 10
Log10 relative expression
Control
HAse
hiHAse
Ccl2
Spp1
Tgfb1
Tgfb3
Il6
C
Hyaluronan polymer n>1000
N-acetylglucosamine
Glucuronic acid
Xylulose
Ascorbic acid
Pentose phosphate pathway
Oxalic acid
Threose
D
relative mRNA/18S
Control
HAse
hiHAse
Threose 0.1mM
Threose 0.5mM
Threose 1mM
Threose 2.5mM
Threose 5mM
Fabp4
Adipoq
Cebpa
Fasn
E
delta osmolarity after 2 days
hiHAse
HAse
Mannitol 0.5%
Mannitol 1%
hiHAse + 0.5% Mannitol
hiHAse + 1% Mannitol
HAse + 0.5% Mannitol
HAse + 1% Mannitol
mOsm
F
Cebpa
Pparg
relative mRNA/18S
Ctrl
Mannitol 0.5%
Mannitol 1%
HAse
HAse+ Mannitol 0.5%
HAse+ Mannitol 1%
hiHAse
hiHAse+ Mannitol 0.5%
hiHAse+ Mannitol 1%
G
Fasn
Cd36
Adipoq
relative mRNA/18S

Figure 3

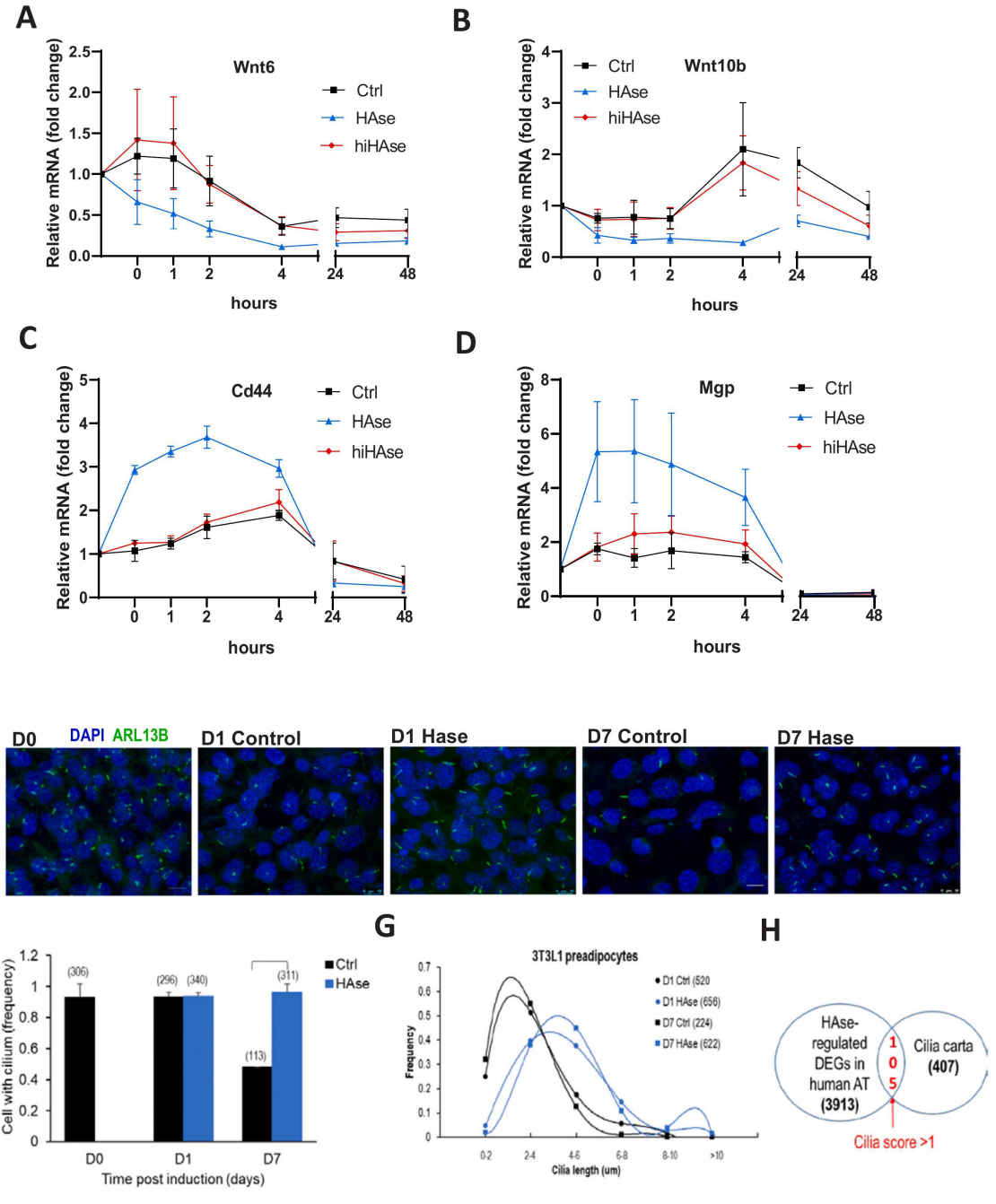
A
Wnt6
Ctrl
HAse
hiHAse
Relative mRNA (fold change)
hours
B
Wnt10b
C
Cd44
D
Mgp
E
D0
DAPI ARL13B
D1 Control
D1 Hase
D7 Control
D7 Hase
F
Cell with cilium (frequency)
Time post induction (days)
G
3T3L1 preadipocytes
D1 Ctrl (520
D1 HAse (656)
D7 Ctrl (224)
D7 HAse (622)
Frequency
Cilia length (um)
H
HAse-regulated DEGs in human AT (3913)
105
Cilia carta (407)
Cilia score >1

Figure 4